International Review of Electrical Engineering (I.R.E.E.), Vol. 5, N. 5
September-October 2010

# Reverse Power Data Analysis and Feature Extraction Based Upon Continuous Wavelet Transform for Electric Power Plants

Sezai Taskin, Serhat Seker, Burak Irgen, Tahir Cetin Akinci

**Abstract** – *This study is focused on the investigating of a power plant generator in reverse power condition. For this purpose, reverse power data were collected from a Combined Heat and Power Plant generator protection relay. The reverse power conditions were evaluated by means of the time-frequency and time-scale methods. As a result of this evaluation, it can be said that the time-frequency and time-scale properties of the signals like current, voltage, frequency, active and reactive powers were extracted with all details.* 

***Keywords**: Power Plants, Generator Protection, Reverse Power, Continuous Wavelet Transform*

## Nomenclature

| | |
|---|---|
| $x(t)$ | Signal |
| $g(t)$ | Fixed dimension window |
| $N$ | Block of data of length |
| $\tau$ | Centered time location |
| $\Delta f$ | Frequency resolution |
| $\Delta t$ | Data-sampling interval |
| $\gamma_{xy}$ | Coherence function |
| $S_{xx}$ | Auto-power spectral density of $x(t)$ |
| $S_{yy}$ | Auto-power spectral density of $y(t)$ |
| $S_{xy}$ | Cross power spectral density between $x(t)$ and $y(t)$ |
| $W_f$ | Continuous wavelet transform of $f(x)$ |
| $\psi(w)$ | Fourier transform of $\psi(x)$ |

## I. Introduction

Localized power sources such as co-generation, wind turbines etc. commonly known as distributed generation. When the distributed generators are operated in parallel with the utility systems, some problems occur due to interconnections such as reverse power flow. Therefore, generators need for maximum protection against the occurring faults [1].

Power generators are important components of an electrical energy system. So, it must be protected in order to maintain the quality and reliability of the power supply. One of the most important components of this system is Digital Fault Recorders (DFRs) [2].

The DFRs have been used commonly, providing valuable means to a deeper analysis of disturbances. When installed in power plants, these devices record sampled waveforms of voltage and current signals, besides the status of relays and other digital quantities related to the generator circuit. Regarding with protection systems, miscellaneous study have been published in the literature [3-5].

In reference [1], an automated scheme to examine digital fault recorder recordings is shown. Another study presents a new wavelet-based negative-phase sequence protection scheme for synchronous generators [6]. Davidson et al. show the application of a multi-agent system to the automatic fault diagnosis of a real transmission system [7]. Luo and Kezunovic's study proposed an expert system that makes use of data from DFRs and sequence of events of digital protection relays to analyze the disturbance and evaluate the protection performance [8]. Styvaktakis et al. have employed a Kalman filter to separate the oscilography into pre-fault, fault and post-fault stages [9].

For this study, reverse power data are collected from Manisa Organized Industrial District (MOSB) Combined Heat and Power Plant, which is located western of Turkey, generator protection relay. This relay is able to detect disturbances and when this occurs, all digital and analog signals are stored in its memory. Data sampling rate for the relay is selected as 10 ms. Total recording time is 7.96 s for pre-fault, fault and post-fault data from abnormal condition of the generator.

## II. Power System Protection

The primary purpose of power system protection is to ensure safe operation of power systems. Furthermore, the task is to minimize the impact of unavoidable faults in the system [10]. In Fig. 1, general schema for protective relaying system consisting of instrument transformers, a relay, and a circuit breaker is shown.

The basic function of an electrical protective relay can be expressed like this: The signal provided by the transducer will be in the form of current or voltage and will be interpreted by the relay as an acceptable level, according to a pre-set value determined by the relay configuration.

*Manuscript received and revised September 2010, accepted October 2010* 

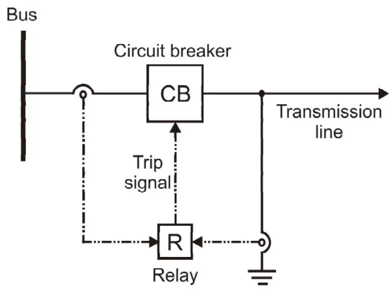


Fig. 1. General protective relaying system [11]

If the pre-set value is exceeded then the relay will initiate further electromechanical action that will often result in disconnection of the electrical machine, and will flag the fact that a fault, or even failure, has been identified [11].

Modern digital relays have a monitoring function. Also, they can record the voltages and currents for a period before and after any fault [12].

### *II.1. Reverse Power Relay Function*

Radial distribution networks are usually designed for unidirectional power flow, from the in feed downstream to the loads. This assumption is reflected in standard protection schemes with directional over current relays. With a generator on the distribution feeder, the load flow situation may be change [13].

The reverse power relay is used to protect a synchronous generator, running in parallel with mains, from motoring mode. Motoring situation occurs due to the failure of the prime mover such as a turbine or an engine driving a generator that is connected to the grid. The generator which is running at the synchronous speed will continue to run at the same speed. However, the power required to keep the generator running along with the prime mover will be drawn from the mains. Therefore, power flows in the reverse direction i.e. bus to the generator. This condition is called as reverse power.

Reverse power operation may be cause damage to the prime mover. Hence, reverse power protection is a vital part of the generator protection scheme.

The reverse power relay operates by measuring the active component of the load current, $I \times \cos\varphi$. When the generator is supplying power, the $I \times \cos\varphi$ is positive, in a reverse power situation it turns negative. If the negative value exceeds the set point of the relay, the relay trips the generator circuit breaker after the preset time delay. The typical setting for reverse power is 4% in case of turbines and 8% in case of diesel engines. The time delay can be set from 2 to 20 seconds [14].

## III. Combined Heat and Power Plants

Combined Heat and Power (CHP) or cogeneration is the simultaneous production of electricity and heat from a single fuel source such as natural gas, biomass, biogas, coal, waste heat, or oil. One of the most common CHP systems is gas turbine or engine with heat recovery unit. Gas turbine or engine CHP systems generate the electricity by burning fuel (natural gas or biogas) and then use a heat recovery unit to capture heat from the combustion system's exhaust stream. This heat is converted into useful thermal energy, usually in the form of steam or hot water [15].

In Fig. 2, a general CHP system block diagram is shown. Here, the output heat of the gas turbine is found in its exhaust. This is a high temperature source and then it can be used to generate high temperature, high pressure steam. This steam will be generated in a waste-heat boiler attached directly to the turbine exhaust [16].

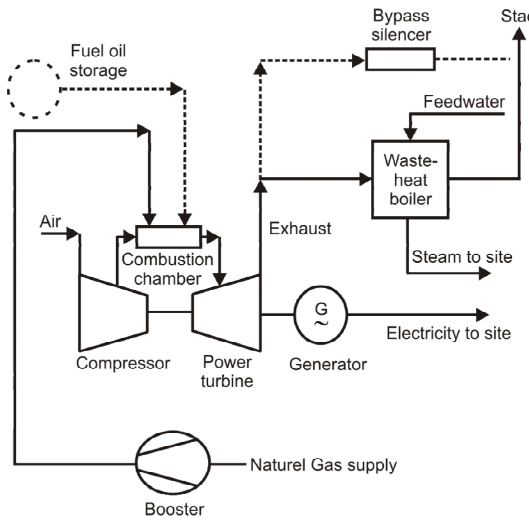


Fig. 2. Block diagram of gas turbine based Combined Heat and Power System [17]

### *III.1. Overview of the Combined Heat and Power Plant*

For this study, reverse power data are collected from the MOSB-Energy CHP Plant. The plant use natural gas for primary energy source.

While three generators 16.638 MW electrical outputs, other five generators have 8.730 MW electrical outputs. The generators deliver electricity through 33 kV transformers to the local grid of the industrial park. The total steam production capacity is around 45 tones/h. Hot water is fed into the district heating system of the industrial park [18].

## IV. Mathematical Methods

In this study, spectral analysis methods are used to reverse power flow analysis for the power plant generator.

For this purpose, power spectral density approach and Short-Time Fourier analysis methods are considered as well as coherence approach.

### *IV.1. Short-Time Fourier Transform and Other Spectral Analysis Methods*

The Short-Time Fourier Transform (STFT) is useful in presenting the time localization of frequency components of signals. The STFT spectrum is obtained by windowing the signal through a fixed dimension window. The signal may be considered approximately stationary in this window. The window dimension fixes both time and frequency resolutions. To define the STFT, let us consider a signal *x(t)* with the assumption that it is stationary when it is windowed through a fixed dimension window g(t), centered at time location τ. The Fourier transform of the windowed signal yields the STFT [19]:

$$STFT(\tau, f) = \int_{-\infty}^{+\infty} x(t)\, g(t-\tau)\, exp[-j2\pi f t]\, dt \quad (1)$$

This equation maps the signal into a two-dimensional function in the time-frequency $(t, f)$ plane. The analysis depends on the chosen window $g(t)$. Once the window $g(t)$ is chosen, the STFT resolution is fixed over the entire time-frequency plane.

A common approach for extracting the information about the frequency features of a random signal is to transform the signal to the frequency domain by computing the Discrete Fourier Transform (DFT). For a block of data of length $N$ samples, the transform at frequency $m\Delta f$ is given by:

$$X(m\Delta f) = \sum_{k=0}^{N-1} x(k\Delta t)\, exp[-j2\pi km / N] \quad (2)$$

where $\Delta f$ is the frequency resolution and $\Delta t$ is the data-sampling interval. The auto-power spectral density (APSD) of $x(t)$ is estimated as:

$$S_{xx}(f) = \frac{1}{N}\left|X(m\Delta f)\right|^2, f = m\Delta f \quad (3)$$

The cross power spectral density (CPSD) between $x(t)$ and $y(t)$ is similarly estimated. The statistical accuracy of the estimate in Equation (3) increases as the number of data points or the number of blocks of data increases.

The cause and effect relationship between two signals or the commonality between them is generally estimated using the coherence function. The coherence function is given by:

$$\gamma_{xy}(f) = \frac{\left|S_{xy}(f)\right|}{\sqrt{S_{xx}(f)\, S_{yy}(f)}}, 0 < \gamma_{xy} < 1 \quad (4)$$

where $S_{xx}$ and $S_{yy}$ are the APSD's of $x(t)$ and $y(t)$, respectively, and $S_{xy}$ is the CPSD between $x(t)$ and $y(t)$. A value of coherence close to unity indicates highly linear and close relationship between the two signals [20,21].

### *IV.2. Wavelet Transform*

The use of wavelet transform is particularly appropriate since it gives information about the signal both in frequency and time domains. Let *f(x)* be the signal, the continuous wavelet transform of *f(x)* is then defined as:

$$W_f(a,b) = \int_{+\infty}^{-\infty} f(x)\, \psi_{a,b}(x)\, dx \quad (5)$$

where:

$$\psi_{a,b}(x) = \frac{1}{\sqrt{|a|}}\psi\left(\frac{x-b}{a}\right) \quad a, b \in R, \quad a \neq 0 \quad (6)$$

and it provides the admissibility condition as below:

$$C_\psi = \int_0^{+\infty} \frac{\left|\psi(\omega)\right|^2}{\omega}\, d\omega < \infty \quad (7)$$

And for this reason:

$$\int_{-\infty}^{+\infty} \psi(x)\, dx = 0 \quad (8)$$

Here $\psi(\omega)$ stands for the Fourier transform of $\psi(x)$. The admissibility condition implies that the Fourier transform of $\psi(x)$ vanishes at the zero frequency. Therefore $\psi$ is called as a wave or the mother wavelet and it have two characteristic parameters, namely, dilation ($a$) and translation ($b$), which vary continuously. The translation parameter, "$b$", controls the position of the wavelet in time. A "narrow" wavelet can access high-frequency information, while a more dilated wavelet can access low-frequency information. This means that the parameter "$a$" varies with different frequency. The parameters "$a$" and "$b$" take discrete values, $a = a_0^j$, $b = nb_0 a_0^j$, where $n, j \in Z$, $a_0 > 1$, and $b_0 > 0$. The discrete wavelet transformation (DWT) is defined as [22]:

$$DWT[j, k] = \frac{1}{\sqrt{a_0^j}} \sum_n f[n]\, \psi\left[\frac{k - na_0^j}{a_0^j}\right] \quad (9)$$

## V. Data Collection System from the Power Plant

In this study "generator protection relay" is used in order to collect the reverse power data. In this sense, the relay is able to detect disturbances and during this case, all digital and analogue signals are stored in its memory, including the pre-fault, fault and post-fault intervals. Disturbance recorder sampling rate is been selected 10o S/s. So, recording time is 7.96 s and also total data number size is 796 S.

In Fig. 3, the generator protection relay connection system is shown as generally.

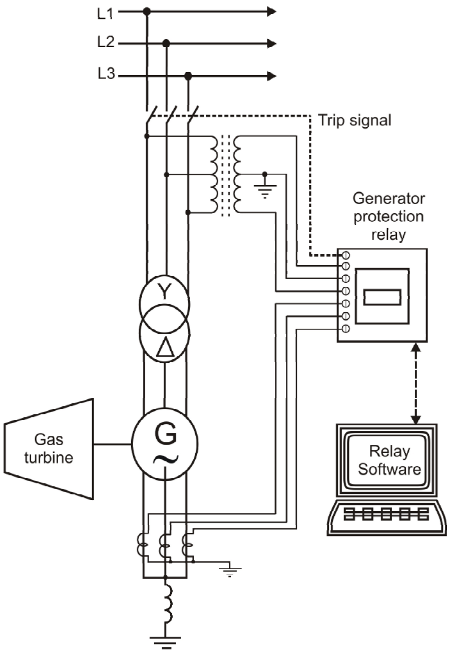


Fig. 3. Generator protection relay connection schema [17]

### *V.1. The Power Plant Generator Specifications*

In Table I, the power plant generator, under the reverse power condition, specifications are given.

TABLE I
THE POWER PLANT GENERATOR SPECIFICATIONS

| | Electrical Parameter | Nominal Value | |
|---|---|---|---|
| 1 | Generator nominal power | 10670 | kVA |
| 2 | Nominal shaft power (Pm) | 8760 | kW |
| 3 | Active Power | 9030 | kW |
| 4 | Reactive Power | 1582 | kVar |
| 5 | Power factor | 0.98 | |
| 6 | Setting for stage P< | -4.0 | %Pm |
| 7 | Setting for stage P<< | -20 | %Pm |

Disturbance recorder parameters and its values for this generator are also shown in Table II.

## VI. Time-Scale and Time-Frequency Analysis for the Reverse Power Data

In this study, the reverse power data, which are collected during the transition case from abnormal condition of the generator to motoring mode, present current, voltage, active and reactive power data as well as frequency variation.

In this sense, the time domain variations related to the reverse power case are shown by the following figures. Here, only one generator, which is given its specifications in Table I, reverse power data is been analyzed.

TABLE II
DISTURBANCE RECORDER PARAMETERS

| | Electrical Measurement Parameter | Value | |
|---|---|---|---|
| 1 | Active Power | 9030 | kW |
| 2 | Reactive Power | 1582 | kVar |
| 3 | Apparent Power | 8518 | kVA |
| 4 | Power Factor | 0.98 | |
| 5 | Frequency | 49.980 | Hz |
| 6 | Phase current IL1 | 437 | A |
| 7 | Phase current IL2 | 435 | A |
| 8 | Phase current IL3 | 440 | A |
| 9 | Io residual current | 0.00 | A |
| 10 | Io2 residual current | 0.000 | A |
| 11 | Line voltage U12 | 11590 | V |
| 12 | Line voltage U23 | 11595 | V |
| 13 | Line voltage U31 | 11600 | V |
| 14 | Phase voltage UL1 | 6695 | V |
| 15 | Phase voltage UL2 | 6700 | V |
| 16 | Phase voltage UL3 | 6705 | V |
| 17 | Residual voltage | 0.0 | % |
| 18 | Unbalance (I2/Igen) | 0.3 | % |
| 19 | Current –seq./+seq. | 0.2 | % |

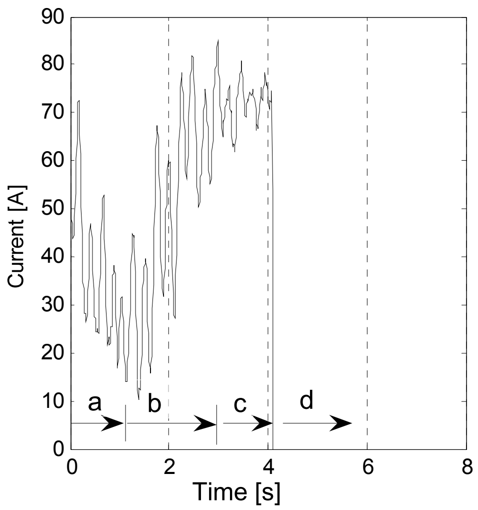


Fig. 4. Current signal variation for line-1 of the generator

As seen in the Fig. 4 the total measurement time is 7.96 s with sampling rate at 100 S/s, for this reason the total number of the data points is 796. Here, four different time-regions are considered.

The first one (a), between the 0 and 1.5 s, indicates the decreasing of the current in generator mode; the second one (b) is related to the motoring mode which is defined between the 1.5 and 3 s; the third one (c) takes place between the 3 and 4 s and it denotes the critical region of the data before the tripping signal of the protection relay. And also, the last one (d) shows the separation region of the generator from the bus bar.

These regional classifications of the data are very important in terms of the feature extraction studies to be used in identifying the relay behavior. In this sense, the third region (c) can be used in emphasizing the spectral characteristics of the relay and hence, some spectral features before the tripping can be determined with all details.

Also voltage variation begins to drop at the tripping time, which is almost around at 4 s. This variation is presented by Fig. 5.

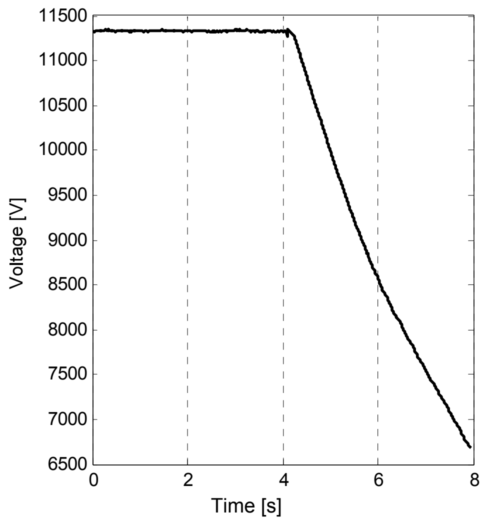


Fig. 5. Voltage variation of the generator

In terms of the active and reactive power variations during the reverse power condition of the generator, the similar findings as obtained from the current waveform are represented by Fig. 6 and Fig. 7. Also, Fig. 8 shows the frequency changes during the reverse power condition.

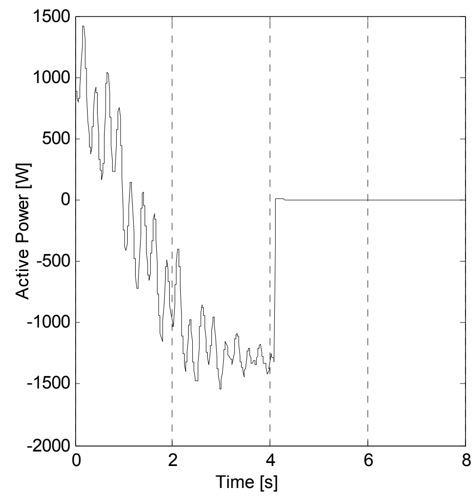


Fig. 6. Active Power variation of the generator

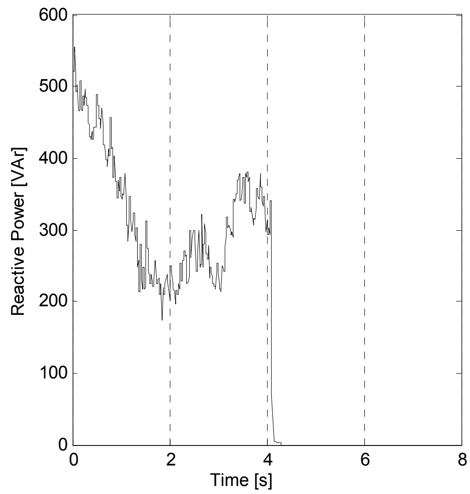


Fig. 7. Reactive power variation of the generator

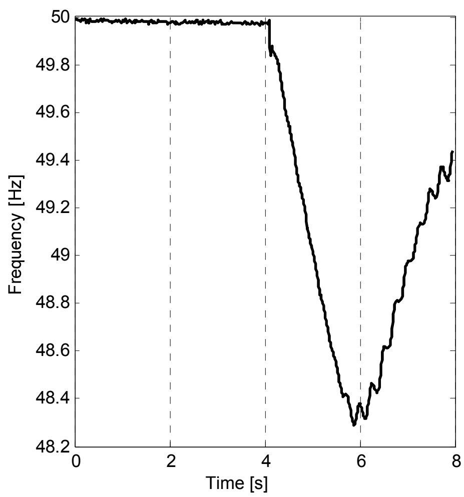


Fig. 8. Frequency variation of the generator

To define the spectral behavior of the relay, time-frequency technique based upon spectrograms can be used and for this purpose, the spectral properties of the tripping duration can be easily determined.

As seen in the Fig. 9, in a very short time, a special frequency band between the 0 and 30 Hz occurs before the tripping. This special frequency band can be defined as a fundamental property of the relay behavior. That effect can be interpreted as a property come from the region (c) indicated in the Fig. 4. As an alternative approach the similar application can be considered for Continuous Wavelet Transform (CWT) and hence it is shown by the following figures.

From the Figs. 10(a) and (b), at the beginning of the reverse power condition, the current contains fluctuation shown by low frequencies between 0-30 Hz, as indicated in the Fig. 9. However, within very short time before the tripping, some high amplitudes begin to appear as a noise characteristic at low frequency region (Fig. 10(b)).

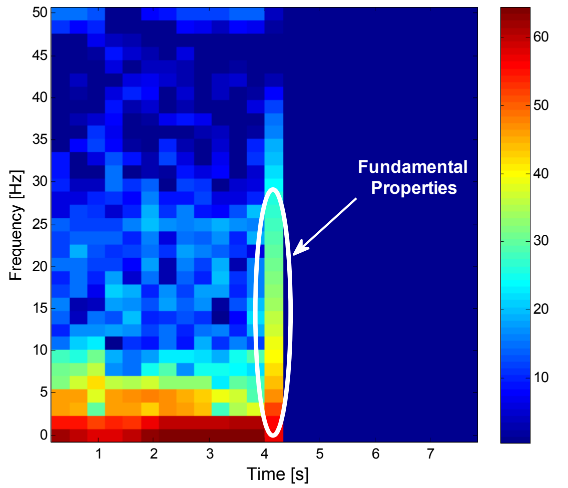


Fig. 9. Time-frequency plot for the generator first phase current

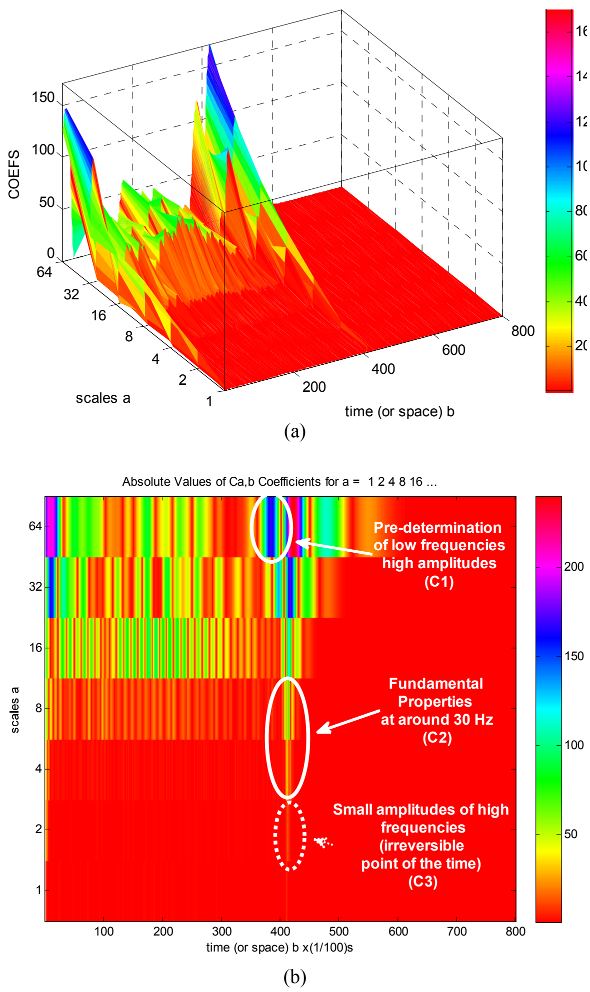


Figs. 10. CWT analysis for current signal of the generator. a) 3D view, b) time-scale presentation

Also, it can be determined that the existence of the small amplitudes with relatively high frequency between 30-50 Hz (Here, "scale a" is proportional with reciprocal of the frequency) within very short time at around 4th second (see Fig. 10(b)).

These are the special characteristics of the protection relay on the time-scale plane. The condition (c3) can be shown on the Fig. 10(b) as irreversible point of the process. Hence, it can be said that the protection relay will send the tripping signal to the circuit breaker. As a comparison of the Figs. 11 and Fig. 10(b), it is seen that the CWT approach is more sensitive than the STFT approach to changes with low frequency and small amplitudes in terms of the proceeding times after the tripping. Here the region (c) of the Fig. 4 can be connected by the pre-determination region (c1) of the Fig. 10(b).

Also, time-frequency and time-scale plots of active power during the reverse power condition for the generator are shown in Figs. 11.

As seen in Figs. 11, it is obtained similar results with the current signals. Also, signal analysis results for reactive power can be shown by means of the Figs. 12.

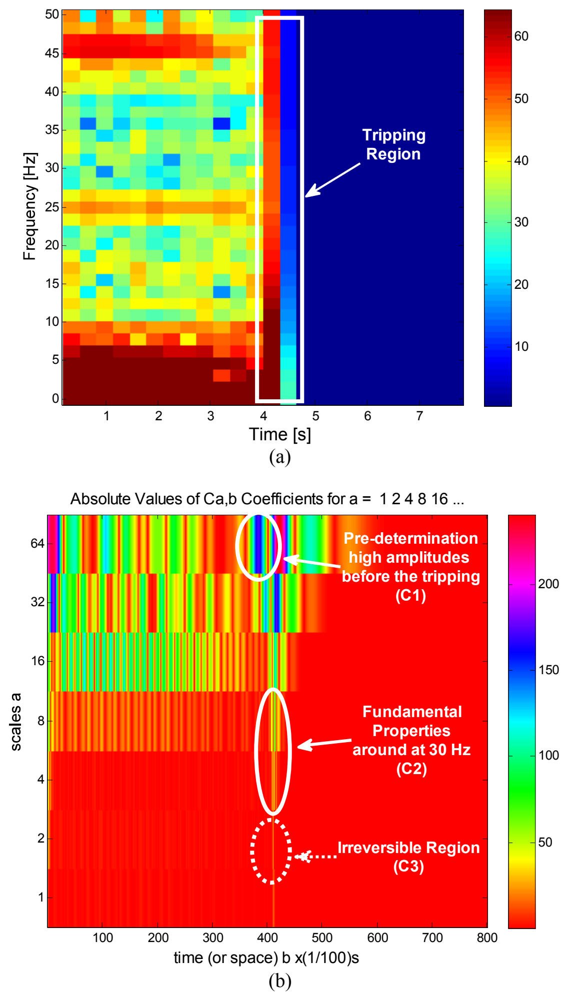


Figs. 11. Active power signal analysis of the generator
a) STFT b) CWT

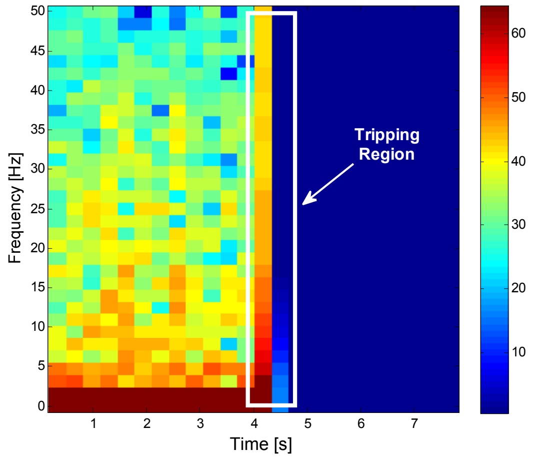


(a)

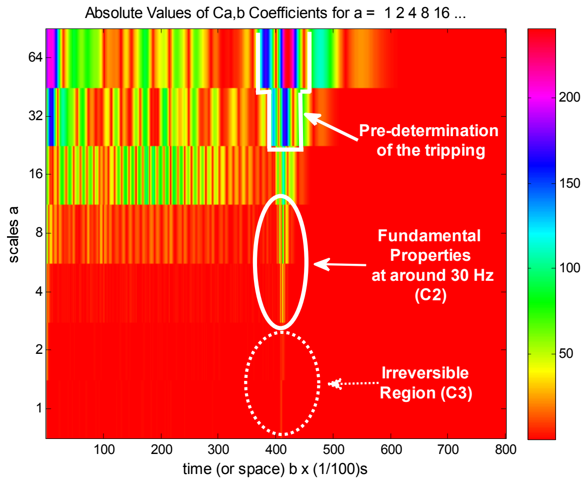


(b)

Figs. 12. Reactive power signal analysis of the generator
a) STFT b) CWT

## VII. Conclusion

In this research, the reverse power conditions were evaluated by means of the time-frequency and time-scale methods. As a result of this evaluation, it can be said that time-frequency and time-scale properties of the signals like current, active and reactive powers were extracted with all details. In this sense, the continuous wavelet transform approach was introduced and its importance was emphasized as a powerful technique because it provides more effective possibility than the Short-Time Fourier analysis in terms of the time-frequency (or time-scale) localization. Hence, with this study, some behavioral properties of the reverse power relay were released by these methods.

General findings related with this research can be listed as below:

1. The CWT analysis is more convenient method than the STFT approach because it decomposes the fundamental properties of the tripping.
2. The decomposed regions on the time-scale plane, which is defined by the CWT, are categorized by the regions (c1), (c2) and (c3).
3. The region (c1) denotes the pre-determination region before the tripping.
4. The region (c2) is related to the fundamental frequency property, which is given at around 30Hz, appeared before tripping time.
5. The region (c3) is an indicator, which occurred around 40 Hz with high frequency components at low amplitude, of the reversible region of the relay during the tripping time. In this manner, it is seen that the STFT approach is insufficient under the comparison with its CWT approach.

## Acknowledgements

Authors present their special thanks to the general manager and technical/engineering units of the Manisa Organized Industrial District Combined Heat and Power Plant (MOSB-Energy) in Turkey for the supports provided during this research.

## References

[1] M. C. Wrinch, *Negative Sequence Impedance Measurement for Distributed Generator Islanding Detection*, The University of British Columbia, Ph.D Thesis, 2008.
[2] M. Moreto and J. G. Rolim, Automated Analysis of Digital Fault Recorder Data in Power Generating Plants, *International Journal of Innovations in Energy Systems and Power*, *vol.3, n. 2*, 2008.
[3] M. Marttila, P. Verho and K. Kannus, Overvoltage Protection Optimization of Medium Voltage Network, *International Review of Electrical Engineering (IREE), vol.3. n.1*, 2008, pp. 17-22.
[4] D. Labed and A. Bouzid, Protection of Dispersed Generation Connected to a Transmission Network, *International Review of Electrical Engineering (IREE), vol. 3. n.4*, 2008, pp. 673-681.
[5] M. A. Omidiora and M. Lehtonen, Protection of Lightning Disturbances on MV Underground Cable, *International Review of Electrical Engineering (IREE), vol. 5. n.1*, 2010, pp. 317-326.
[6] O.A.S. Youssef, A Wavelet-based Approach for Protection of Generators Against Unbalanced Currents, *Electric Power Systems Research*, *vol. 63, n.1*, 2002, pp. 73-80.
[7] E.M. Davidson, S.D.J. McArthur, J.R. McDonald, T. Cumming and I. Watt, Applying Multi-agent System Technology in Practice: Automated Management and Analysis of SCADA and Digital Fault Recorder Data, *IEEE Transactions on Power Systems*, *vol. 21, n. 2,* 2006.
[8] X. Luo and M. Kezunovic, *Fault Analysis Based on Integration of Digital Relay and DFR Data*, IEEE Power Engineering Society General Meeting Document, San Francisco, USA, 2005.
[9] E. Styvaktakis, M.H.J. Bolen and I.Y.H. Gu, Expert System for Classification and Analysis of Power System Events, *IEEE Transactions on Power Delivery, vol. 17, n. 2,* 2002, pp.423-428.
[10] M. Geidl, *Protection of Power Systems with Distributed Generation: State of the Art*, Swiss Federal Institute of Technology (ETH), Power Systems Laboratory Reports, July 2005.
[11] J.L. Blackburn and T.J. Domin, *Protective Relaying: Principles and Applications*, CRC Press, 2007.
[12] P.J. Tavner, L. Ran, J. Penman and H. Sedding, Condition Monitoring of Rotating Electrical Machines, *IET Power and Energy Series, 56,* United Kingdam, 2008.
[13] J.A.P. Lopes, Integration of Dispersed Generation on Distribution Networks Impact Studies, *IEEE Power Engineering Society*, *vol.1,* 2002, pp. 323-328.

[14] L. L. Grigsby, *Electric Power Generation, Transmission, and Distribution,* CRC Press; 2nd edition, 2007.
[15] *Combined Heat and Power: A Clean, Local Energy Solution*, Energy Matters, 2009.
[16] Wartsila Company Brochure, *Combined Heat and Power Plants*, www.wartsila.com, April 2009.
[17] S. Taskin, Power Plants Monitoring for Reverse Power Flow Evaluation, *Istanbul University - Journal of Electrical & Electronics Engineering (IU-JEEE), Issue 19, Volume 10, Number 1,* 2010 (In Press).
[18] P.A. Breeze, *Power Generation Technologies*, Newnes Book, 2005, p. 69
[19] S. Taskin, S. Seker, M. Karahan and C. Akinci, Spectral Analysis for Current and Temperature Measurements in Power Cables *Electric Power Components and Systems*, *vol.37, n.4,* 2009, pp. 415-426.
[20] S. Seker and E. Ayaz, A Reliability Model for Induction Motor Ball Bearing Degradation, *Electric Power Components and Systems*, *vol.31,n.7,* 2003, pp. 639-652.
[21] S. Seker, Determination of Air-gap Eccentricity in Electric Motors Using Coherence Analysis, *IEEE Power Engineering Review*, *vol. 20, n. 7,* 2000, pp. 48-50.
[22] E. Onal, O. Kalenderli and S. Seker, De-noising Technique Based on Wavelet Decomposition for Impulse Voltage Measurements and Noise Analysis, *International Review of Electrical Engineering* (*I.R.E.E.*)*, vol.* 5*, n.* 3, 2010, pp. 1789-1797.


## Authors' information

**Sezai Taşkın** received his B.Sc., M.Sc. and Ph.D. degrees from the Marmara University (MU), Electrical Education Department, in 1999, 2001 and 2007 respectively. He is currently assistant professor of control and automation department at Celal Bayar University. His research interests have been focused on power system analysis, signal processing applications and mechatronic systems.

**Serhat Şeker** received his B.Sc., M.Sc. and Ph.D., degrees from the Istanbul Technical University (ITU), Electrical Engineering Department, in 1985, 1988 and 1995 respectively. In 1990 and 1994, he worked in Signal Analysis Group at the Netherlands Energy Research Centre-ECN. Between 1997 and 1998, he joined to Nuclear Engineering Department and Maintenance & Reliability Centre (MRC) at the University of Tennessee-Knoxville (UT). He is currently professor of electrical engineering at ITU. His research interests are signal processing, soft computing and condition monitoring techniques.

**Burak İrgen** received his B.Sc., degree from the Dokuz Eylul University, Electrical and Electronics Engineering Department, in 2000. In 2001, he worked in DEMAS-İzmir as construction chief of High Voltage Transmission Lines in Mediterranean Region. Currently, he is Automation and Control Systems Engineer in MOSB Energy Cogeneration Power Plant in Manisa Organized Industrial District.

**Tahir Çetin Akıncı** received his B.Sc. degree from the Fırat University in 2000, M.Sc. and Ph.D degrees from the Marmara University (MU), Electrical Education Department, in 2005 and 2010 respectively. He is an assistant professor at Kırklareli University. His research interests have been focused on control systems, power system analysis and signal processing applications.